IOPscience iopscience.iop.org

Home Search Collections Journals About Contact us My IOPscience

Solvent effects on ^{13}C and ^{15}N shielding tensors of nitroimidazoles in the condensed phase: a sequential molecular dynamics/quantum mechanics study

This article has been downloaded from IOPscience. Please scroll down to see the full text article.

2004 J. Phys.: Condens. Matter 16 6159

(http://iopscience.iop.org/0953-8984/16/34/015)

View the table of contents for this issue, or go to the journal homepage for more

Download details:
IP Address: 129.252.86.83
The article was downloaded on 27/05/2010 at 17:15

Please note that terms and conditions apply.

INSTITUTE OF PHYSICS PUBLISHING JOURNAL OF PHYSICS: CONDENSED MATTER

J. Phys.: Condens. Matter **16** (2004) 6159–6170 PII: S0953-8984(04)78082-0

Solvent effects on ^{13}C and ^{15}N shielding tensors of nitroimidazoles in the condensed phase: a sequential molecular dynamics/quantum mechanics study

Teodorico C Ramalho[1], **Elaine F F da Cunha**[2] **and Ricardo Bicca de Alencastro**[2]

[1] Max-Planck-Institut für Kohlenforschung, Kaiser-Wilhelm-Platz 1, D-45470 Mülheim an der Ruhr, Germany
[2] Physical Organic Chemistry Group, Departamento de Química Orgânica, Instituto de Química, Universidade Federal do Rio de Janeiro, Ilha do Fundão, CT, Bloco A, Laboratory 609, 21949-900, Rio de Janeiro-RJ, Brazil

E-mail: teo@ime.eb.br

Received 17 March 2004
Published 13 August 2004
Online at stacks.iop.org/JPhysCM/16/6159
doi:10.1088/0953-8984/16/34/015

Abstract

^{15}N and ^{13}C NMR chemical shifts for three nitroimidazoles have been calculated and compared with experimental data. The solvent effects on NMR spectra were simulated with the polarizable continuum model (PCM) and an alternative sequential molecular dynamics/quantum mechanics methodology (S-MD/QM). The sampling of the structures for the quantum mechanical calculations is made by using the interval of statistical correlation obtained from the auto-correlation function of the energy. Magnetic shielding tensors were evaluated at the GIAO-B3LYP level using II′ basis set. It has been shown that it is essential to incorporate the dynamics and solvent effects in NMR calculations in the condensed phase.

1. Introduction

Nowadays, the most used radiosensitizers are the nitroimidazole derivatives [1, 2]. Recently, ^{1}H, ^{31}P and ^{19}F NMR/MRI (magnetic resonance imaging) [3] of nitroimidazoles has been applied for measuring tumour [4] and tissue oxygenation [5]. In spite of their great importance, the solvent effects on the NMR parameters of such radiosensitizers have not been investigated so far. In recent years there has been an increasing interest in the description of solvent effects on molecular properties [6–9]. The theoretical description of the solute–solvent interaction and its influence on solute properties is of central concern in theoretical physical chemistry. The solute–solvent interaction is usually treated on the bases of electrostatic, induction and dispersion forces [8, 9]. Specific interactions, such as hydrogen bonding, are treated with

 © 2004 IOP Publishing Ltd Printed in the UK

special attention; this interaction is of interest in a variety of processes and is of special concern in biophysical systems. More recently, the hybrid quantum mechanical/molecular mechanics (QM/MM) approach has emerged as a powerful method for studying shielding tensors in the condensed phase [10, 11]. In such a procedure the solute molecule (or the portion of the system that needs a QM description) is treated quantum mechanically, while the remainder of the system (solvent molecules) is represented by classical force fields. These two subsystems communicate through electrostatic and van der Waals interactions terms. In this approach, electronic structure calculations are carried out during the simulation; energy and its derivatives for the quantum system are also obtained. The QM/MM approach has been implemented with both Monte Carlo [11] and molecular dynamics methods [12]. As many configurations are generated in a sufficiently large MD, then the number of QM calculations required in a hybrid QM/MM–MD simulation is too high, since in every step an energy evaluation of the system is needed. So, great computational effort is necessary to carry out this kind of simulation. Aiming at reducing the computational demand, some inexpensive QM methods, such as valence-bond [10] and semi-empirical molecular orbital methods [12], can be considered. However, for some classes of compounds, for example transition metals compounds, these approximate molecular orbital method are not appropriate due to the lack of parameters [13–15].

The sequential MD/QM procedure differs from the conventional QM/MM–MD method [10, 12] in that all molecules (solute and solvent) are treated by quantum mechanics. The classical MD part of S-MD/QM is used only to generate the statistical structure of the liquid. Another important point is that all statistical information is obtained before running the QM stage. In a previous study [16] we have shown the applicability of using molecular dynamics (MD) followed by quantum mechanical (QM) calculations (S-MD/QM) to the calculation of NMR parameters for guanylhydrazone in aprotic solvents.

Whereas the shielding tensor calculation has been employed in various systems [16–18], little attention has been given to this type of calculation in flexible molecules in solution. This work was devoted to theoretical studies of ^{13}C and ^{15}N NMR chemical shifts of 4-nitroimidazoles (figure 1) in the condensed phase, using molecular dynamics (MD) followed by quantum mechanical (QM) calculations (S-MD/QM). In addition, the calculated ^{15}N and ^{13}C chemical shifts are compared with experimental data and with PCM methodology.

2. Computational procedures

2.1. opt-PCM/DFT methodology

The conformers from the gas phase were optimized with B3LYP/6-311++G** using the polarized continuum model (PCM) [8]. The chosen radii to form the molecular cavity are 1.9 Å for the aromatic carbons bonded to a hydrogen atom, 1.6 Å for all nitrogen atoms, 1.52 Å for oxygen and 1.2 Å for the hydrogens of H-bonded water. All the radii have been multiplied by a factor (1.2 if not otherwise specified) in order to take into account the fact that atomic bonds or lone pair centres of the solvent molecules are normally located a bit farther from solute atoms than the van der Waals radius [19, 20]. After each optimization, a constant force calculation was carried out. The shielding tensor was obtained using GIAO and the gradient-corrected density functional Becke's three-parameter Lee, Yang and Parr (B3LYP) exchange functional [21] with the basis set II′ [22] in the *Gaussian98 A.11* software package [23]. All the ^{13}C chemical shifts are referenced to those of benzene (128.5 ppm), while the ^{15}N chemical shifts are referenced to nitromethane (0.0 ppm). The absolute ^{13}C shielding of benzene and ^{15}N shielding of nitromethane was calculated at the B3LYP/ II′ level on the B3LYP/6-311++G** optimized geometries.

2.2. S-MD/QM methodology

All molecular mechanics calculations were carried out with the Insight/Discover program (version 2.9.7) using the consistent valence force field (CVFF) [24] for both solute and solvent. As usual, periodic boundary conditions (PBC) and a cutoff distance of 9.0 Å have been applied [25]. The system consists of 254 TIP3P [25] water molecules in a cubic cell with a side of 20 Å. The volume of the cube was determined by the density of the liquid water ($\rho = 0.996$ g cm^{-3}). The MD simulations were performed at 298 K. The constant atom number, temperature and volume (*NVT*) ensemble, known as the canonical ensemble, was applied. The Verlet Leapfrog method [26] was used to integrate the equations of motion with time steps of 1 fs. First, the initial configuration was minimized using the steepest descent and the conjugate gradient algorithm until an energy gradient of 0.01 kcal mol^{-1} Å^{-1} was reached. The desired molecular properties were calculated from molecular dynamics simulations using the CVFF force field [24]. The simulation consisted of a thermalization stage of 500 ps, followed by an additional period of 1 ns. Furthermore, the uncorrelated configurations were selected from statistical inefficiency calculations [16] using SciLab 2.7 software [27]. Finally, the structures obtained from the MD simulations were used for the QM calculations [23] of the chemical shifts. The GIAO method [28], using density functional theory with the B3LYP method at the II′ level, was employed for the chemical shift calculations. ^{13}C and ^{15}N chemical shifts are referenced in the same way as PCM calculations. The basis set superposition error (BSSE) for the complexation-induced results was estimated using the counterpoise correction method [29].

3. Results and discussion

3.1. Chemical shift analysis using opt-PCM/DFT

The elected methodology, which was used as the standard methodology in our study, was *opt*-PCM/DFT (PCM-B3LYP/6-311++G**). Among other basis sets, the choice of the basis set 6-311++G** improved the results, so that they are completely satisfactory. The 6-311++G** basis set has been shown to be satisfactory on similar structures [8, 14]. The smaller basis sets are unsatisfactory and the higher ones are too expensive. A significant difference between theory and experiment was seen in N-3 and N-1 and in the carbons CH_2Y and C-5 of all studied compounds when we use just B3LYP/6-311++G** on the optimization steps. In fact, the results using *opt*-PCM/DFT when compared with these obtained without considering the solvent effect (optimization in vacuum—*opt*-DFT) are significantly better, showing the convenience of including this effect on the optimization steps (tables 1 and 2).

To take into account the gauge-origin problem, we used the gauge-including atomic orbital (GIAO) method at the density functional level of theory [28] in each selected conformation. Accordingly, using the PCM-B3LYP/6-311++G** level of calculations, the most significant errors in the NMR calculations B3LYP/ II′ levels were 15.9 ppm for ^{15}N chemical shifts (**2**) and 7.28 ppm for ^{13}C chemical shifts (**3**). The results are summarized in tables 1 and 2. The greatest error on the ^{15}N chemical shifts appears for (**3**): 15.9 ppm for N-3, and 9.7 for N-1. This is followed by 15.6 for N-3 and 8.1 ppm for N-1 (**2**) and 15.4 for N-3 and 7.4 for N-1 ppm (**1**). N-3 shows a higher error for all compounds due to its higher sensibility to the solvent effects (H-bonding).

Also, the shifts computed for the carbon atoms appear at considerably higher fields than those measured experimentally, with an error around 1.80 and 7.28 ppm. The greatest error in ^{13}C chemical shifts is observed for the carbon bond to the hydroxyl group in compound (**3**)

Table 1. ^{15}N NMR experimental [18] and theoretical chemical shift data (ppm) for the nitroimidazoles.

Compound		N-1	N-3
1	Experimental	−208.5	−127.7
	opt-DFT	−193.0	−98.7
	opt-PCM/DFT	−201.1	−112.3
	S-MD/QM	−206.8	−124.5
2	Experimental	−203.3	−132.0
	opt-DFT	−186.7	−101.9
	opt-PCM/DFT	−195.2	−116.1
	S-MD/QM	−205.9	−129.2
3	Experimental	−205.7	−131.7
	opt-DFT	−189.2	−102.7
	opt-PCM/DFT	−196.2	−116.1
	S-MD/QM	−203.6	−128.4

Table 2. ^{13}C NMR experimental [17] and theoretical chemical shift data (ppm) for nitroimidazoles.

Compound		C-2	C-4	C-5	CH_3	CH_2Y
1	Experimental	138.60	147.80	123.10	13.35	—
	opt-DFT	140.80	152.10	130.99	15.03	—
	opt-PCM/DFT	140.40	151.80	127.30	14.70	—
	S-MD/QM	139.80	148.19	123.92	14.31	—
2[a]	Experimental	145.69	145.46	122.44	12.75	49.38
	opt-DFT	152.72	149.56	131.09	15.20	59.39
	opt-PCM/DFT	152.19	149.26	128.24	15.05	56.63
	S-MD/QM	146.89	146.03	123.82	13.85	51.56
3[b]	Experimental	145.16	145.76	121.79	12.05	47.76
	opt-DFT	151.91	149.61	130.96	14.06	58.04
	opt-PCM/DFT	151.36	149.36	128.96	13.96	55.04
	S-MD/QM	146.39	146.27	123.21	13.23	49.78

[a] Y = $CH(OH)CH_3$.
[b] Y = $CH(OH)CH_2Cl$.

(7.28 ppm). The chemical shifts calculated for this carbon in the series are 7.28 and 7.20 ppm for (**3**) and (**2**), respectively (table 2). These pronounced greater errors for the chemical shifts of atoms on the side chain, may be due to higher structural flexibility of this part of molecule in solution.

The chemical shifts for all the nuclei on the aromatic ring are in good agreement with the calculated data. The comparison of the average error for the rigid part of the molecule (the imidazole ring) with the average error for the flexible part of the molecule (the side chain) shows that the smallest errors are found for the rigid part, thus indicating that the conventional theoretical methodology used does not evaluate the chemical shifts of the flexible part of the molecule with appropriate accuracy.

3.2. Chemical shift analysis using S-MD/QM

3.2.1. Statistical correlation. The average value of a property such as the energy of a molecular system corresponds to a simple average over a group of size L of instantaneous

values, as shown in equation (1).

$$\langle E\rangle_L = \frac{1}{L}\sum_i^L E_i. \tag{1}$$

When L is large enough, the average value of the property converges and, because of the finite size of the simulation, it is given by

$$\sigma(\langle E\rangle_L) = \sqrt{\frac{\langle E^2\rangle - \langle E\rangle^2}{L-1}}. \tag{2}$$

Successive configurations are usually not independent, because each molecule has attempted to move only once. Therefore, it is necessary to calculate the interval of the uncorrelated configurations to have statistical efficiency in the calculation of the average properties and to calculate the statistical error properly.

There are two independent methods for calculating the interval of uncorrelated configurations. One method uses the auto-correlation function of the energy to obtain the correlation step τ [25] and the other uses the statistical inefficiency s [31]. The auto-correlation function $C(n)$ is given by

$$C(n) = \frac{\langle \delta E_i \delta E_{i+n}\rangle}{\langle \delta E^2\rangle}. \tag{3}$$

It is known that, for Markovian processes, $C(n)$ has an exponential decay [30, 31] as given in equation (4).

$$C(n) = \sum_{i=1}^{N} c_i \mathrm{e}^{-n/\tau_i}. \tag{4}$$

The interval between uncorrelated configurations, or the correlation step τ, is calculated by integration from zero to infinity of $C(n)$. In practice, configurations separated by 2τ, or larger intervals, are considered uncorrelated.

The statistical inefficiency (equation (5)) is based on the mean-square deviations of averages taken over blocks of a group of configurations. The limiting value s signifies that the nth block has become so large that there is no correlation from block to block. Thus, the configurations separated by intervals larger than s are uncorrelated.

$$s = \lim_{n\to\infty} \frac{n\langle \delta E^2\rangle_n}{\langle \delta E^2\rangle}. \tag{5}$$

These two methods for calculating the interval of uncorrelated configurations are independent; however they are related by $s = 2\tau$ [32].

Both methods have already been used to improve the calculation of some thermodynamic properties such as pressure [33], chemical potential [34] and equilibrium constant [34]. In the early work [16] we have used them to obtain uncorrelated configurations in order to reduce the number of structures used in the NMR calculations. These configurations were obtained from the correlation step calculations using the auto-correlation function of the energy. Figure 2 shows the calculated auto-correlation function versus simulation time for (**3**). Integrating the best fit, we obtained the correlation steps (τ) and the statistical inefficiencies (s) from equation (4). The exponential decays that best fit the values for all the studied compounds give very similar results for τ for the compounds (**1**), (**2**) and (**3**) around 9.97 and 11.05 and 11.90 ps, respectively.

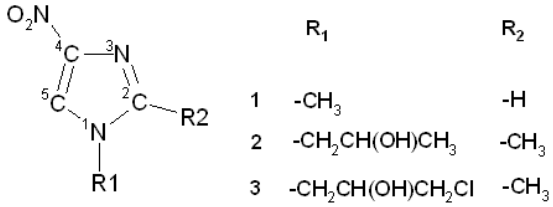

Figure 1. Compounds used in work.

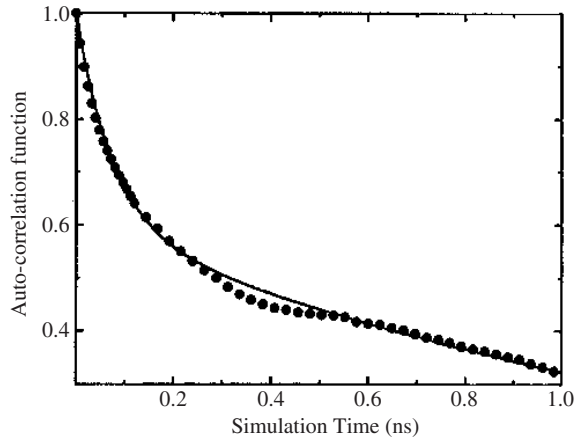

Figure 2. Calculated auto-correlation function of the energy for (**3**) in water.

3.2.2. Radial pair distribution function. An important point in the solvation of a radiosensitizer in water is the formation of hydrogen bonds. For example, the radial pair distribution function between N-3 of (**3**) and the water hydrogen, $g_{N-H}(r)$, is shown in figure 3(A), and the radial pair distribution function between the oxygen of (**3**) and the water hydrogen, $g_{O-H}(r)$, is shown in figure 3(B). This information will be used in this work to define in a consistent way the size of the cluster used in the QM calculation. Hydrogen-bonded structures are conventionally obtained from the analysis of the radial distribution pair function $g_{N-H}(r)$ and $g_{O-H}(r)$, which is shown in figure 3 [25]. A well-defined first peak centred at ca 2.50 Å is observed for $g_{N-H}(r)$, locating the first minimum at 4.2 Å. The spherical integration of the first peak gives 1.2 water molecules as nearest neighbours. For $g_{O-H}(r)$, a first peak centred at about 1.55 Å is observed, locating the first minimum at 2.55 Å. The spherical integration of the first peak gives 0.9 water molecules as nearest neighbours.

With the information supplied from the computer RDFs, the selection of the solvent molecules included in a given cluster is done on the basis of a cutoff distance (r_{cut}) for N–H and O–H pairs: all solvent molecules having the hydrogen atom closer than r_{cut} to the solute (either nitrogen or oxygen) will be included in the NMR calculation of the corresponding structures [35]. The value used for r_{cut} for the N–H pair was 4.20 Å for all compounds and 2.55 Å for O–H for (**2**) and (**3**). Hydrogen bonds in liquids are better obtained using geometric and energetic criteria, as discussed before by Stilinger and Rahamn [36]. Indeed, these are more appropriate for studying solvent effects in spectroscopy [37]. In addition to r_{cut}, we consider here a hydrogen-bond formation when the distance $R_{DA} < 4$ Å, the angle AHD $< 30°$ and the binding energy is higher than 3.0 kcal mol^{-1}. The sampling of the structures for the quantum

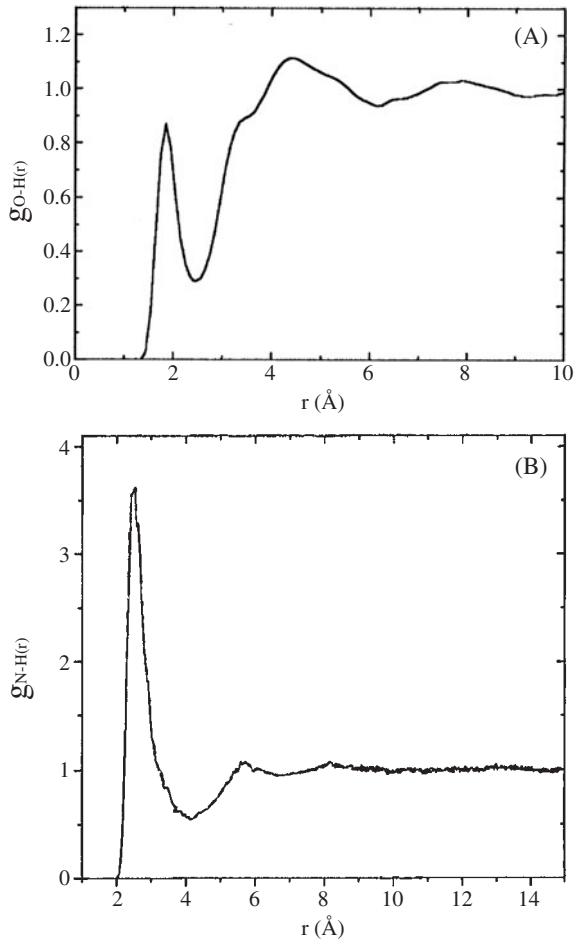

Figure 3. (A) Radial pair distribution function between the nitrogen atom of (**3**) and the oxygen atom of water. (B) Radial pair distribution function between the oxygen atom of (**3**) and the hydrogen of water.

mechanical calculations is made by using the interval of statistical correlation obtained from the auto-correlation function of the energy from molecular dynamics simulation.

3.2.3. Chemical shift analysis—S-MD/QM methodology. Using the S-MD/QM methodology the error on the calculated chemical shifts for the compounds studied was less than 3.3 and 2.18 ppm for ^{15}N and ^{13}C, respectively. This larger error for ^{15}N can be explained on the basis of the greater dependence of the chemical shift of this nucleus on solvent effects as compared to ^{13}C chemical shifts.

Analysis of the results for N-3 in all compounds shows an error close to 3.0 ppm. We clearly observe a better prediction of the chemical shift of this atom when the calculation was carried out using the *opt*-PCM/DFT and *opt*-DFT methodologies (around 17.8 and 30.0 ppm, respectively).

The largest observed ^{15}N chemical shift deviation error is 3.3 ppm for N-3 in (**3**) and 2.6 ppm for N-1 in (**2**).

For the carbon bonded to the hydroxyl group (CH) the calculated data show an error of 2.18 ppm for (**2**) and about 2.02 ppm for (**3**). These calculated chemical shifts were better predicted by S-MD/QM methodology (calculated values around 50.67 ppm and experimental chemical shifts around 48.57 ppm). The chemical shifts calculated for all the nuclei in the imidazole ring are in good agreement with the experimental data.

For both ^{15}N and ^{13}C nuclei in the flexible and rigid parts of the molecules studied, the S-MD/QM methodology showed much better agreement with the experimental values than the usual methodology (*opt*-PCM/DFT).

We can observe that the use of the S-MD/QM methodology evaluated the chemical shifts of the atoms at the flexible part of the molecules with accuracy. We believe that this methodology gives a good correlation between theoretical and experimental results when used on flexible molecules in solution.

3.2.4. Shield tensor calculation—S-MD/QM methodology. The choice of nitrogen as the NMR active nucleus has been induced by a good knowledge of its shielding sensitivity to changes in the environment [8, 20]. In our methodology, S-MD/QM, the structures were generated in large MD simulations using PBC conditions and explicit water molecules to evaluate the solvent effect. To take into account the BSSE problem, we used the counterpoise correction [29, 38]. The results obtained from S-MD/QM methodology are shown in tables 1 and 2, where the greatest error is about 3.3 ppm for nitrogen nuclei and 2.18 ppm for carbon nuclei.

The theoretical methodologies used to describe the solvent effect on the spectroscopic properties of molecules can be classified into groups [39–41]: discrete cluster models [39, 42], continuum models [43, 44], and molecular dynamics, either classical or quantum [45–49]. In this paper, we have investigated the solvent effects on the shielding tensor with different approaches. For the MD approach, we have applied an appropriate statistical criterion to select the snapshots employed in the QM calculation.

There are other details that are important when using only the solvation continuum model for shield tensor calculations. For example, the cavity size effect is an important aspect that has led to many different studies of a systematic nature [8]. In QM calculations one of the most used solvation continuum models is the polarized continuum model (PCM) [50]. In its original version, PCM defines the cavity as an envelope of spheres centred on atoms (or at most atomic groups) [50, 51]. The problem is shifted to the size of the spheres, whereas several studies have shown that standard van der Waals radii provide reasonable cavity sizes [52]. This situation results in difficulties with the continuum model representing some apolar solvents, for example cyclohexane [35]. Furthermore, a single optimization step is not adequate to explore the conformational space of a molecule in solution [53–55]. The real situation is of a dynamic nature, and a variety of different and representative structures can and do occur. The inclusion of molecular dynamics is important to reproduce the behaviour of molecules in a condensed phase, where average properties and not properties of a single structure (minimum of the potential energy surface) are obtained. In this work 42 configurations were selected in agreement with statistical inefficiency calculations. Furthermore, an accurate description of H-bond effects on nuclear shielding is possible though clusters formed by solute and some solvent molecules. The statistical inefficiency and correlation time values were calculated as described previously. It is well known that the correlation time is inversely proportional to molecular mobility [56]. Then, based on the statistical inefficiency calculation for (**3**), 42 configurations were selected for all the compounds. (**3**) shows the greatest correlation time, followed by (**2**). (**1**) shows a smaller correlation time and therefore a greater number of uncorrelated configurations. Since (**3**) gave the smallest ensemble, using the number of

uncorrelated configurations of this compound for the other two guarantees the calculation of the chemical shifts only for uncorrelated structures for the three compounds. It can be observed that the correlation time of the system increases as the molecular volume of the radiosensitizer decreases.

The results obtained with *opt*-PCM/DFT have shown the necessity of introducing other interactions, in particular those deriving from short-range specific effects induced by H-bonding. The difference between *opt*-PCM/DFT and S-MD/QM methodologies results can be explained by high sensitivity of the shielding on molecular geometries; also, small differences in bond lengths and angles can induce large variations in the shield tensor. Moreover, the use of explicit solvent molecules coordinating directly with the solute induces changes in terms of the valence natural population, due to electron transfer between the atoms N and O of the solute and solvent molecules, which influences strongly the electron density near the O, N and H involved in H-bonding.

3.2.5. Statistical convergence. This procedure described below was chosen to perform the conformational search due to the complex landscape of minima presented by flexible molecules [53–55]. We chose ^{15}N NMR as the parameter to evaluate the effect of the number of selected structures from the MD simulation, because ^{15}N is more sensitive to changes in the molecular environment than ^{13}C NMR [57]. In this study, the statistical inefficiency (s) calculation was used as the criterion to select conformations from the MD simulation. However, in order to check the influence of the number of structures (N) selected from the MD calculation on the chemical shift, we changed N and carried out chemical shift calculations with 1, 14 ($N = \frac{1}{3}s$), 21 ($N = \frac{1}{2}s$), 42 ($N = s$), 84 ($N = 2s$) and 126 ($N = 3s$) structures from the MD simulation. According to figure 4, in the case of (**2**), it can be observed that the absolute error in the chemical shift decreases dramatically with the number of selected conformations from the MD simulation. It can be seen that, from $N = 42$ to 126, there is only a slight decrease in the absolute error in the calculated chemical shift, as compared with the error variation for values of $N < 42$. It seems that $N = 42$ is one inflexion point, which represents the most appropriate selection choice in terms of cost/benefit. For N values greater than 42 there is only a slight improvement in the calculated ^{15}N chemical shifts, with, however, a much greater computational demand.

In order to check the influence of the number of selected structures (N) for the other compounds ((**1**) and (**3**)), N-3 was chosen. This selection was made considering that N-3 shows the greatest absolute error when comparing the calculated with the experimental data (see figure 4). The results are shown in figure 4, which shows that the absolute chemical shift error decreases dramatically with the increase of N. This behaviour was also observed previously [16, 30]. This result shows that configurations separated by 2τ contribute significantly to the average, while using configurations separated by $<2\tau$ may be a wasted effort, as this leads to inclusion of configurations that do not contribute to the average.

4. Concluding remarks

In summary, the results obtained considering the solvent effect are significantly better than those obtained from optimization in vacuum (*opt*-DFT), showing the convenience of including this effect in NMR calculations. From our results, it is evident that the use of an S-MD/QM methodology for the calculation of ^{13}C and ^{15}N chemical shifts affords superior results when compared with the usual methodology (*opt*-PCM/DFT). In fact, all the data calculated with S-MD/QM were closer to the experimental data, especially for ^{15}N chemical shifts, which are

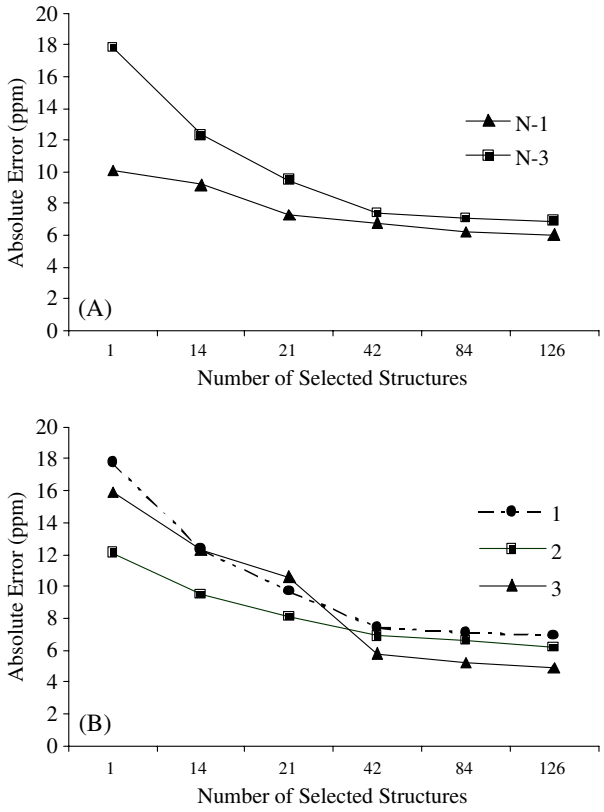

Figure 4. (A) Number of selected configuration from MD calculations and absolute error in the chemical shift for (**3**). (B) Number of selected configuration from MD calculations and absolute error in the chemical shift for all compounds.

nuclei with greater sensitivity to changes in the molecular environment than ^{13}C. It can also be concluded that the S-MD/QM methodology is noticeably better than the *opt*-PCM/DFT methodology for the flexible parts of the molecule. This result stresses the importance of taking into account the dynamics of the problem. The methodology presented here can clearly be applied for the estimation of other simulations and other systems. The present application demonstrates the feasibility of this approach. In addition, running the MD simulation first gives important statistical information that is fundamental for subsequent QM calculations. It is important to stress that the dynamic contribution should be accounted for by selecting an appropriate ensemble of statistically independent conformations. In this way the configuration generated in the simulation can be drastically reduced without loss of statistical information. To our knowledge, this is the first application of this methodology to NMR parameters in the condensed phase.

Acknowledgments

We are grateful to both Brazilian and Germanic agencies, FAPERJ and CAPES and DAAD respectively, for funding part of this work. We are especially grateful to Dr Ahmet Altun for his comments and suggestions on the manuscript.

References

[1] Hori H, Jin C Z, Kiyono M, Kasai S, Shimamura M and Inayama S 1997 *Bioorg. Med. Chem.* **5** 591
[2] Chapman J D, Coia L R, Stobe C C, Engelhart E L, Fenning M C and Schneider R F 1996 *Br. J. Cancer* **74** S204
[3] Lauffer R B 1987 *Chem. Rev.* **87** 901
[4] Anderson C J and Welch M J 1999 *Chem. Rev.* **99** 2219
[5] McCoz C L, McIntire D J O, Robinson S P, Aboagze O E and Griffiths J R 1996 *Br. J. Cancer* **74** S226
[6] Reichardt C 1979 *Solvents and Solvent Effects in Organic Chemistry* (Weinheim: Verlag-Chemie)
[7] Warshel A 1991 *Computer Modeling of Chemical Reactions in Enzymes and Solutions* (New York: Wiley)
[8] Tomasi J and Persico M 1994 *Chem. Rev.* **94** 2027
[9] Cramer C J and Truhlar D G 1995 *Reviews in Computational Chemistry* vol 6, ed D B Boyd and K B Lipkowitz (New York: VCH)
[10] Segall M D 2002 *J. Phys.: Condens. Matter* **14** 2957
[11] Cui Q and Karplus M 2000 *J. Phys. Chem.* B **104** 3721
[12] Field M J, Bash P A and Karplus M 1990 *J. Comput. Chem.* **11** 700
[13] Ramalho T C and Figueroa-Villar J D 2002 *J. Mol. Struct. (Theochem)* **580** 217
[14] Ramalho T C, Martins T L C and Figueroa-Villar J D 2003 *Int. J. Quantum Chem.* **95** 267
[15] Ramalho T C, Cunha E F F and Alencastro R B 2004 *J. Mol. Struct. (Theochem)* **676** 149
[16] Ramalho T C, Martins T L C and Figueroa-Villar J D 2003 *Magn. Reson. Chem.* **41** 983
[17] Mckillp A, Wright D E, Podmore M L and Chambers R K 1983 *Tetrahedron* **39** 3797
[18] Chen B C, Philipsborn W and Nagarajan K 1983 *Helv. Chim. Acta* **146** 1537
[19] Bondi A 1964 *J. Phys. Chem.* **68** 441
[20] Mennucci B 2002 *J. Am. Chem. Soc.* **124** 1506
[21] Wang P, ZhangY L and Streitwieser A 1991 *J. Am. Chem. Soc.* **113** 55
[22] Kutzelnigg W, Fluscher U and Schindler M 1999 *The IGLO-Method Ab Initio Calculation and Interpretation of NMR Chemical Shift and Magnetic Susceptibilities* vol 23 (Heidelberg: Springer)
[23] Frisch M J, Trucks G W, Schlegel H B, Scuseria G E, Robb M A, Cheeseman J R, Zakrzewski V G, Montgomery J A Jr, Stratmann R E, Burant J C, Dapprich S, Millam J M, Daniels A D, Kudin K N, Strain M C, Farkas O, Tomasi J, Barone V, Cossi M, Cammi R, Mennucci B, Pomelli C, Adamo C, Clifford S, Ochterski J, Petersson G A, Ayala P Y, Cui Q, Morokuma K, Salvador P, Dannenberg J J, Malick D K, Rabuck A D, Raghavachari K, Foresman J B, Cioslowski J, Ortiz J V, Baboul A G, Stefanov B B, Liu G, Liashenko A, Piskorz P, Komaromi I, Gomperts R, Martin R L, Fox D J, Keith T, Al-Laham M A, Peng C Y, Nanayakkara A, Challacombe M, Gill P M W, Johnson B, Chen W, Wong M W, Andres J L, Gonzalez C, Head-Gordon M, Replogle E S and Pople J A 2001 *Gaussian98 A.11 Software Package* (Pittsburgh, PA: Gaussian)
[24] Dauber-Osgutorpe P, Roberts V A and Osgutorpe D G 1988 *Proteins* **4** 31
[25] Allen M P and Tildesley D J 1987 *Computer Simulation of Liquids* (Oxford: Oxford University Press)
[26] Verlet L 1993 *Phys. Rev.* **159** 98
[27] SciLab v 2.7. 1989–2003 INRIA/ENPC
[28] Wolinski K, Hilton J F and Pulay P 1990 *J. Am. Chem. Soc.* **112** 8251
[29] Pecul M, Lewandiwski J and Sadlej J 2001 *Chem. Phys. Lett.* **333** 139
[30] Malaspina T, Coutinho K and Canuto S 2002 *J. Chem. Phys.* **117** 1692
[31] Chafield C 1984 *The Analysis of Times Series: an Introduction* (London: Chapman and Hall)
[32] Friedberg R and Cameron J E 1970 *J. Chem. Phys.* **52** 6049
[33] Fincham D, Quirke N and Tildesley D J 1986 *J. Chem. Phys.* **84** 4535
[34] Swope W C, Andersen H C, Berens P H and Wilson K R 1982 *J. Chem. Phys.* **76** 637
[35] Mennucci B, Martinez J M and Tomasi J 2001 *J. Phys. Chem.* A **105** 7287
[36] Stilinger F H and Rahman A 1974 *J. Chem. Phys.* **74** 3336
[37] Jorgensen W L, Chandrasekhar J, Madura J D, Impey R W and Klein M L 1983 *J. Chem. Phys.* **79** 926
[38] Pecul M and Sadlej J 1999 *Chem. Phys.* **248** 27
[39] Cossi M and Crescenzi O 2003 *J. Chem. Phys.* **118** 8863
[40] Miertus S, Scrocco E and Tomasi J 1981 *J. Chem. Phys.* **55** 117
[41] Pivnenko N S, Drushlyak T G, Kutulya L A, Vashchenko V V, Doroshenko A O and Goodby J W 2002 *Magn. Reson. Chem.* **40** 566
[42] Chesnut D B and Rusiloski B E 1994 *J. Mol. Struct. (Theochem)* **314** 19
[43] Cossi M and Crescenzi O 2004 *Theor. Chem. Acc.* **111** 162
[44] Ruud K, Frediani L, Cammi R and Mennucci B 2003 *Int. J. Mol. Sci.* **4** 119

[45] Odelius M, Laaksonen A, Levitt M H and Kowalewski J 1993 *J. Magn. Reson.* A **105** 289
[46] Malkin V G, Malkina O L, Steinebrunner G and Huber H 1996 *Chem. Eur. J.* **2** 452
[47] Pfrommer B G, Mauri F and Louie S G 2000 *J. Am. Chem. Soc.* **122** 123
[48] Laaksonen A, Stilbs P and Wasylishen R E 1998 *J. Chem. Phys.* **108** 455
[49] Parrinello M and Sebastiani D 2001 *J. Phys. Chem.* A **105** 1951
[50] Barone V, Cossi M and Tomasi J 1998 *J. Comput. Chem.* **19** 404
[51] Cossi M, Barone V and Tomasi J 1998 *Chem. Phys. Lett.* **253** 286
[52] Luque F J, Bash M, Alemn C and Orozco M 1996 *J. Comput. Chem.* **17** 806
[53] Orozco M and Luque F J 1996 *J. Comput. Chem.* **17** 806
[54] Ramalho T C, Figueroa-Villar J D, La-Scalea M A and Alencastro R B 2004 *Biophys. Chem.* **110** 267
[55] Ramalho T C, Cunha E F F and Alencastro R B 2004 *J. Theor. Comput. Chem.* **3** 1
[56] Tinoco L W and Figueroa-Villar J D 1999 *J. Braz. Chem. Soc.* **10** 281
[57] Harris C D 1996 *Quantitative Chemical Analysis* (New York: Freeman)